Conference on Modelling Fluid Flow (CMFF'09)
The 14th International Conference on Fluid Flow Technologies
Budapest, Hungary, September 9-12, 2009

SIMULATION OF THE FLOW AND ACOUSTIC FIELD OF A FAN

Qin Wang[1], Michael Hess, Berthold Matyschok, Peter Pelz

[1] Corresponding Author. Department of Mechanical Engineering, Chair of Fluid Systems Technology
Technische Universität Darmstadt, Petersenstr. 30, 64287 Darmstadt, Germany. E-mail: qin.wang@fst.tu-darmstadt.de

ABSTRACT

The focus of the present work is the steady and unsteady numerical simulation of flow field and flow-induced acoustic field of a fan using a hybrid approach. The steady simulation of the flow field is carried out with a realizable k-epsilon turbulence model. In a second step the result are used for the evaluation of the acoustic sources, which are used as input data of the Broadband Noise Model. From this computational acoustics (CA) we get a qualitative map of acoustic power level in the entire computational domain. From steady flow fields with different mass flows as inlet boundary condition the characteristic curve of the fan (pressure vs. mass flow) is evaluated.

In the unsteady simulation, the acoustic noise propagation is computed using the Ffowcs Williams and Hawkings (FW-H) analogy. The source term in the acoustic propagation equation is achieved from the CFD result. With this unsteady simulation the transient acoustic power level in every location can be calculated, which enables a FFT-analysis of the acoustic field.

Keywords: axial fan, computational fluid dynamics (CFD), computational acoustics (CA), acoustic analogy.

NOMENCLATURE

Z_{IB}	[-]	number of impeller blades
Z_g	[-]	number of guide vane
f_z	[Hz]	frequency
n	[s^{-1}]	rotational speed
ρ	[kg/m^3]	fluid density
ρ_0	[kg/m^3]	unperturbed fluid density
ρ'	[kg/m^3]	fluid density perturbation
t	[s]	reception time
τ	[s]	emission time
H_{ij}	[-]	Heaviside function
$\delta(f)$	[-]	Dirac delta function
p_0	[Pa]	pressure of the undisturbed medium
p'	[Pa]	sound pressure
p_t	[Pa]	total pressure
P_{ij}	[Pa]	compressive stress tensor
T_{ij}	[kg/ms^2]	Lighthill stress tensor
τ_{gap}	[-]	dimensionless gap width
s	[m]	gap width
D_{IB}	[m]	diameter impeller blades
C_μ	[-]	constant
ψ	[-]	dimensionless total pressure rise
ψ_{ideal}	[-]	dimensionless ideal total pressure rise
ψ_V	[-]	dimensionless total pressure rise loss
φ	[-]	dimensionless volume flux
$\underline{u}$	[m/s]	fluid velocity
$\underline{v}$	[m/s]	surface velocity
r	[m]	distance from source to observer
M	[-]	mach number
Q	[m^3/s]	volume flux
η	[-]	efficiency
S_Ω	[s^{-1}]	deformation tensor
S_{ij}	[s^{-1}]	mean rate of strain tensor

1. INTRODUCTION

The acoustic emission of fans is a considerable noise source in cooling system. Noise from axial fan arises mainly due to the turbulent flow around fan blades (broadband) and interaction of propeller and for example guide vane or support struts (tonal). The latter one is dependent on the mounting arrangement of the fan blades. The fan blades are in most cases equidistant in circumferential direction and cause discrete frequency component and its harmonics with $i = 1 \cdots m$ in each rotation, which depend on the speed and the number of the propeller blades:

$$f_z = i\, Z_{IB} n \,.$$

For axial fans the amplitudes according to f_z increases due to interaction of the propeller and guide vane or support struts. Blade number ratios Z_{IB} / Z_g of 1 and 0.5 are to be avoided, otherwise tonal sound power level would strongly increase. In this work the investigated fan has 9 impeller blades and 13 guide vanes.

In the design phase it is important to have a clear picture of the expected hydrodynamic and acoustic performance of the fan. To achieve this, a hybrid method is recommended. One possible hybrid method among others is to use CFD in the near-field provides input data for a acoustic integral formulation to calculate radiated noise. In this work a steady state CFD analysis of an axial fan is carried out to get the characteristic curve and the broadband noise emission of the fan. A unsteady state flow simulation is carried out for the CA using the FW-H analogy [1], which is based on Lighthill's Acoustic Analogy (LAA) [2] derived from the conservation equation of mass and momentum.

2. PROBLEM FORMULATION

The investigated axial fan contains suction and pressure channel on the left and right side respectively. Air is sucked by the fan through the inlet nozzle followed by the anechoic channel and suction channel. On the pressure side at the end of the anechoic channel a choke serves for adjusting the fan working points. The total sound power is measured in the suction channel and pressure channel. The fan has a 0.3% relative gap, defined as $\tau_{gap} = s / D_{IB}$. The rotational speed n was kept constant at 41.67 s^{-1}.

3. THE HYBRID APPROACH

3.1 Flow field

The flow field is modelled with the realizable k-epsilon two equation turbulence model [3] for the Reynolds-averaged Navier-Stokes (RANS) equation. This model contains a transport equation for the dissipation rate based on the dynamic equation of the mean-square vorticityfluctuation and a formulation for the turbulent viscosity μ_t involving a variable C_μ which ensures the positive normal stresses. It is mathematically described by the following equations (1-2):

$$\frac{\partial}{\partial t}(\rho k)+\frac{\partial}{\partial x_j}(\rho k u_j)=\frac{\partial}{\partial x_j}\left[\left(\mu+\frac{\mu_t}{\sigma_k}\right)\frac{\partial k}{\partial x_j}\right]+ G_k+G_b-\rho\varepsilon-Y_M+S_k \quad (1)$$

$$\frac{\partial}{\partial t}(\rho \varepsilon)+\frac{\partial}{\partial x_j}(\rho \varepsilon u_j)=\frac{\partial}{\partial x_j}\left[\left(\mu+\frac{\mu_t}{\sigma_\varepsilon}\right)\frac{\partial \varepsilon}{\partial x_j}\right]+ \rho C_1 S_\varepsilon-\rho C_2\frac{\varepsilon^2}{k+\sqrt{v\varepsilon}}+C_{1\varepsilon}\frac{\varepsilon}{k}C_{3\varepsilon}G_b+S_\varepsilon \quad (2)$$

with

$$C_1 = max\left[0.43, \frac{\eta}{\eta+5}\right],$$

$$\eta = S_\Omega \frac{k}{\varepsilon},$$

$$S_\Omega = \sqrt{2S_{ij}S_{ij}}$$

$$S_{ij} = \frac{1}{2}\left(\frac{\partial u_j}{\partial x_i}+\frac{\partial u_i}{\partial x_j}\right)$$

In these equations, G_k and G_b denotes the generation of turbulence kinetic energy due to the mean velocity gradients and buoyancy respectively. Y_M represents the contribution of the fluctuating dilatation in compressible turbulence to the overall dissipation rate. C_2 and $C_{1\varepsilon}$ are constants. σ_k and σ_ε are the turbulent Prandtl numbers respectively for k and ε . S_k and S_ε are user-defined source terms.

3.2 Acoustic field

3.2.1 Broadband model

Direct simulation and acoustic analogy methods are very time expensive. For design purpose a detailed acoustic information is often not needed, so that broadband models can be sufficient. Broadband models require only information extracted from steady RANS calculations (mean flow field, turbulent kinetic energy k, and the dissipation rate ε). The sound energy is distributed over a broad range of frequencies.

The first type of a broadband models is derived by Proudman [4] for isotropic turbulence noise (quadrupole sources) using Lighthill's acoustic analogy. An other type of the broadband models is based on the Lighthill-Curle's [5] equation for dipole noise, which arises in turbulent boundary layer near a solid body surface. The broadband models are developed for specific problems and not applicable in general. They are limited to the broadband noise characteristics prediction and do not provide any tonal information.

3.2.2 The FW- H integral methods

The Lighthill equation is only applicable to cases without a body within the fluid. Curle [5] extended the Lighthill equation to overcome this restrict. Later Ffowcs Williams-Hawkings (FW-H) [1] extended the Lighthill-Curle's equation further and provided a standard approach for the prediction of noise originated from rotating blades.

More recently, using the so called permeable surface formulation, the FW-H equation is capable to predict the sound generated by equivalent acoustic sources such as monopoles, dipoles and quadrupoles. Assuming a surface $S: f(\vec{x},t)=0$ to be a close moving surface permeable to the fluid, in which every interaction of solid surface and the

fluid enclosed (Fig. 1). The function f is defined as $f<0$ inside S, $f>0$ outside S and $\nabla f=\vec{n}$, with which the normal vector can be calculated.

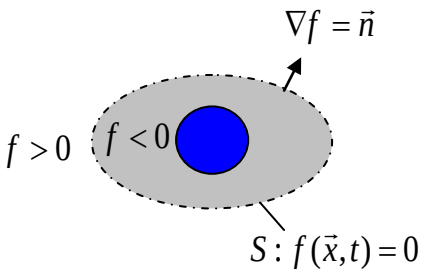

Figure 1. The permeable integration surface

According to Fig. 1 FW-H [1] extends the Lighthill's acoustic equation by combining mass and momentum equations of fluid mechanics using the Heaviside function $H(f)$ to the following equation:

$$\begin{aligned}&\frac{1}{a_0^2}\frac{\partial^2 p'}{\partial t^2}-\nabla^2 p'=\\&\frac{\partial}{\partial t}\{[\rho(u_n-v_n)+\rho_0 v_n]\delta(f)\}-\\&\frac{\partial}{\partial x_i}\{[P_{ij}n_j+\rho u_i(u_n-v_n)]\delta(f)\}+\\&\frac{\partial^2}{\partial x_i x_j}\{T_{ij}H(f)\}\end{aligned} \tag{3}$$

The right-hand side in equation (3) are source terms for the wave equation. The first two terms on the right-hand side are the thickness, loading noise sources respectively and behave like monopole and dipole source term. The last term is a volume term, which is called quadrupole source term distributed in the aerodynamic field exterior to source (emission) surface, and is the double divergence of the Lighthill's stress tensor:

$$T_{ij}=\rho u_i u_j+P_{ij}-a_0^2(\rho-\rho_0)\delta_{ij} \tag{4}$$

with

$$P_{ij}=p\delta_{ij}-\mu\left[\frac{\partial u_i}{\partial x_j}+\frac{\partial u_j}{\partial x_i}-\frac{2}{3}\frac{\partial u_k}{\partial x_k}\delta_{ij}\right] \tag{5}$$

One can get Reynolds stress tensor $\rho u_i' u_j'$ from time-averaged Lighthill's stress tensor .

Because of propagation effect on the radiation path between the sources of the perturbations and the observer, all the right-hand side source terms are generally negligible outside a limited domain (source domain). By integration of equation (3), the first and second term lead to a surface integral while the third terms leads to a volume integral on a region of space V outside of to the integration surface. When $f=0$ coincides with the body surface, using the impermeability condition $u_n=v_n$ and the Green's function and neglecting the quadrupole source term, equation (3) leads to the following integral form.

$$\begin{aligned}&4\pi p'(\vec{x},t)=\\&\int_{f=0}\left[\frac{\rho_0\dot{U}_n+U\dot{n}}{r(1-M_r)^2}\right]_\tau dS+\\&\int_{f=0}\left[\frac{\rho_0 U_n\{r\dot{M}_r+a_0(M_r-M^2)\}}{r^2(1-M_r)^3}\right]_\tau dS+\\&\frac{1}{a_0}\int_{f=0}\left[\frac{\dot{L}_r}{r(1-M_r)^2}\right]_\tau dS+\\&\int_{f=0}\left[\frac{L_r-L_M}{r^2(1-M_r)^2}\right]_\tau dS+\\&\frac{1}{a_0}\int_{f=0}\left[\frac{L_r\{r\dot{M}_r+a_0(M_r-M^2)\}}{r^2(1-M_r)^3}\right]_\tau dS\end{aligned} \tag{6}$$

where $\tau=t-r/a_0$ and

$$\begin{aligned}U_i&=v_i+\rho/\rho_0(u_i-v_i)\\L_i&=P_{ij}\hat{n}_j+\rho u_i(u_n-v_n)\end{aligned} \tag{7}$$

This acoustic formulation is based on Farassat's [6] 1A solution of the FW-H equation. The 1A formulation is a solution of the FW-H equation for thickness and loading noise sources obtained by integration on the body surface and neglecting the quadrupole term. The FW-H analogy is widely used for linear aero-acoustic problems such as the flow through fan impeller. The important limitation of the FW-H analogy in FLUENT 6.3.26 [7] is that it does not account any effect of the flow on propagating sound.

4. SIMULATION SETUP

In the channel, hexahedral elements are used for the mesh. Around the fan tetraeder elements are used to refine the mesh for capturing the flow field more exactly. The mesh consists of 13.7eG elements.

The inlet is defined as a massflow inlet and the outlet is specified as a pressure outlet. The fan is modelled with the frozen-rotor approach for steady state simulation and sliding mesh approach for unsteady state simulation.

The material data of air density of 1.225 kg/m^3 and a dynamic viscosity of 1.78940e-5 Pa.s are used. The fluid is dealed as incompressible.

5. RESULTS – COMPARISON WITH EXPERIMENT

The simulations are carried out with FLUENT 6.3.26. Each steady state simulation run takes approximately 4 days and the transient simulations 7 days on a Intel XEON-processors with 2 Quad-cores machine running Linux.

Fig. 2 shows the total pressure rise achieved from steady state simulation, in comparison with experiment data gained by Karstadt [9]. It shows ideal total pressure rise (ψ_{ideal}) and total pressure rise loss (ψ_V)– all variables are in relation to the efficiency optimum. The difference between the calculated/experimental data and this ideal one is pressure rise loss. The dimensionless total pressure rise and mass flux are defined as follows:

$$\varphi = \frac{4Q}{\pi^2 D_{IB}^3 n}$$
$$\psi = \frac{2\Delta p_t}{\rho \pi^2 D_{IB}^2 n^2} \qquad (8)$$

From the measured or simulated values the ideal curve and the pressure loss is gained

$$\psi_{ideal} = \frac{\psi}{\eta}, \qquad \psi_V = \psi_{ideal} - \psi. \qquad (9)$$

There is a clear difference between the computation and measurements what represents an average difference of about 10% in total pressure rise. The curves of ideal total pressure rise from simulation and experiment should be theoreticaly identical. The difference of these two curves is due to error in simulation and in experiment as well.

In comparison to experiment, larger total pressure rise and lower total pressure rise loss are achieved from simulation. The reasons for this difference are as follows:

a) There is a small different angle of guide vane between simulation and experiment.

b) The used turbulence model is realizable k-epsilon model. In this model C_μ, used for calculation turbulent viscosity μ_t, is not a constant as in the standard k-epsilon [8] model, but a function of the mean strain, rotation rates, the angular velocity of the system rotation, and the turbulence fields (k and epsilon). C_μ includes a term of the angular velocity due to the system rotation. According to [7] simulation with this term is only tested for single rotating reference frame. However, it has been multi rotating reference frame system in this work, in which this turbulence model produces non-physical turbulent viscosities.

c) The unsteady flow is simplified as steady flow in the simulation to save CPU-time.

Fig. 3 shows the efficiency in comparison with experiment data. The difference between these two curves is about 5%.

Fig. 4 shows the results of turbulence intensity which is defined as:

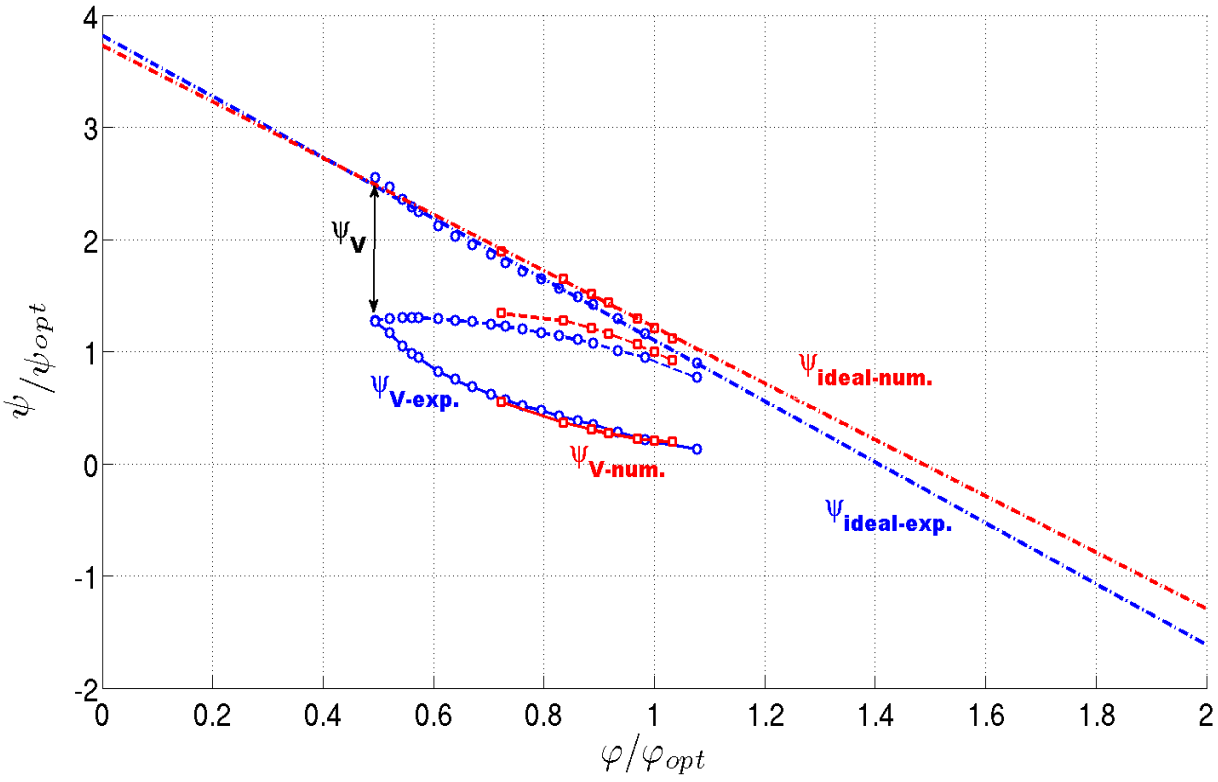

Figure 2. Ideal total pressure rise and total pressure rise loss

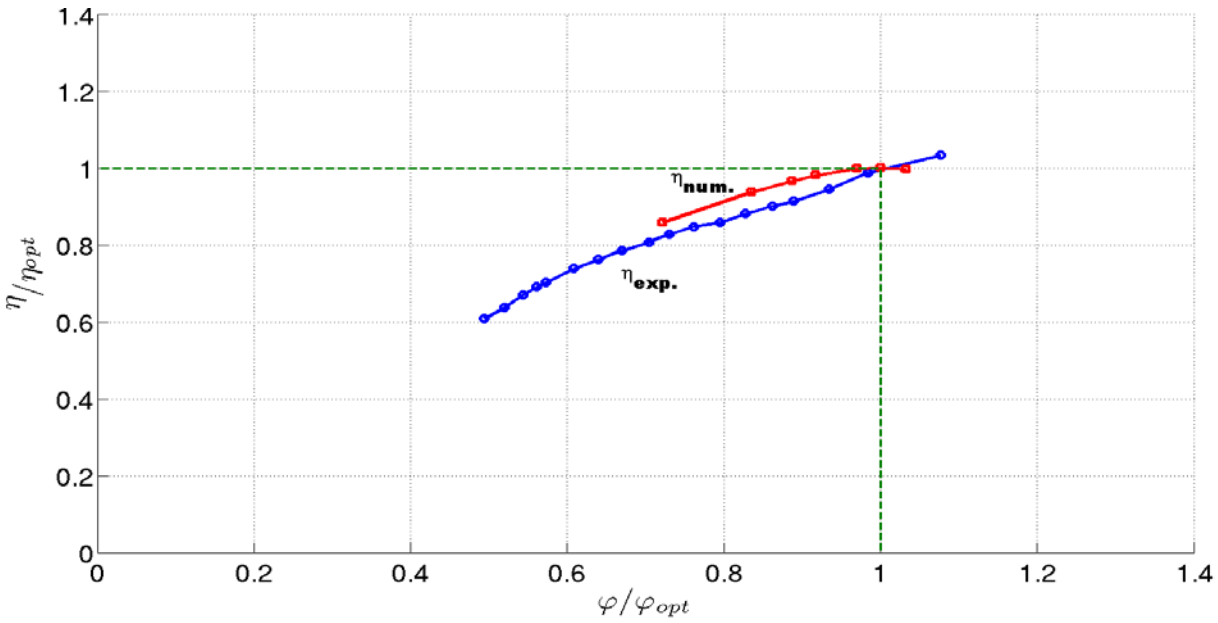

Figure 3. Efficiency in comparison with experiment

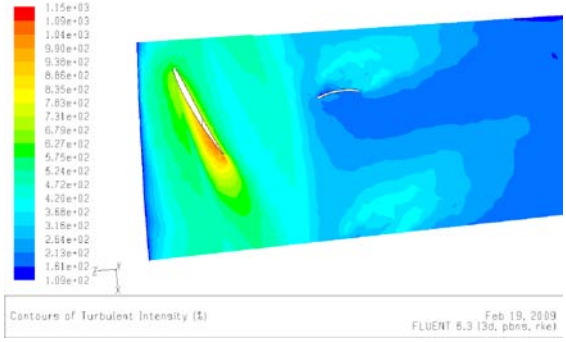

Figure 4. Turbulent intensity around the impeller and guide vane

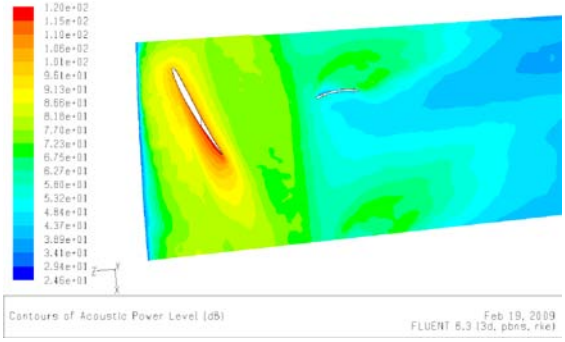

Figure 5. Broadband noise around the impeller and guide vane

$$I = \frac{\sqrt{\frac{2}{3}k}}{U}, \qquad (10)$$

with U the mean velocity (Reynolds averaged) and k turbulent kinetic energy, which is spur of Reynolds stress tensor, achieved from CFD.

This turbulence intensity is decisive for the broadband noise level presented in Fig. 5. Similar contour can be found in Fig. 4 and Fig. 5. The unsteady state results with FW-H analogy are presented in Fig. 6. f_z and its harmonics are qualitatively correct. The source surface f(x, t) = 0 is located on the solid body surface and quadrupole

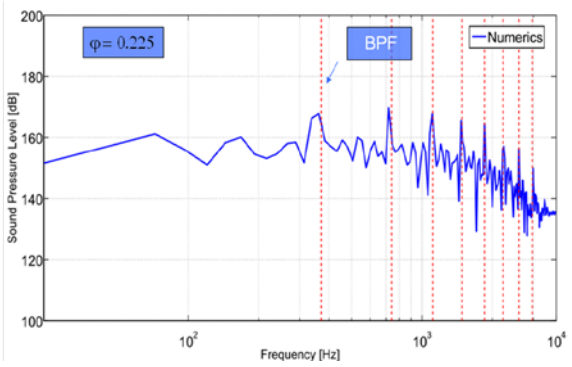

Figure 6. Spectrum of noise in source domain

source term is neglected. Neglecting the quadrupole term is a practical approximation, because the volume integration is very time consuming and this terms are only important for trans/super-sonic flows [10].

Simulations with refined grid show no noticeable difference in total pressure rise (Fig. 7).

6. CONCLUSIONS

In the present work fluiddynamics and acoustics of a fan have been studied.

Total pressure rises simulated with the commercial CFD program FLUENT agree reasonable well with experiment in stationary state. With the broadband model acoustical calculation gives only qualitative results due to its physical formulation (steady state, realizable k-epsilon

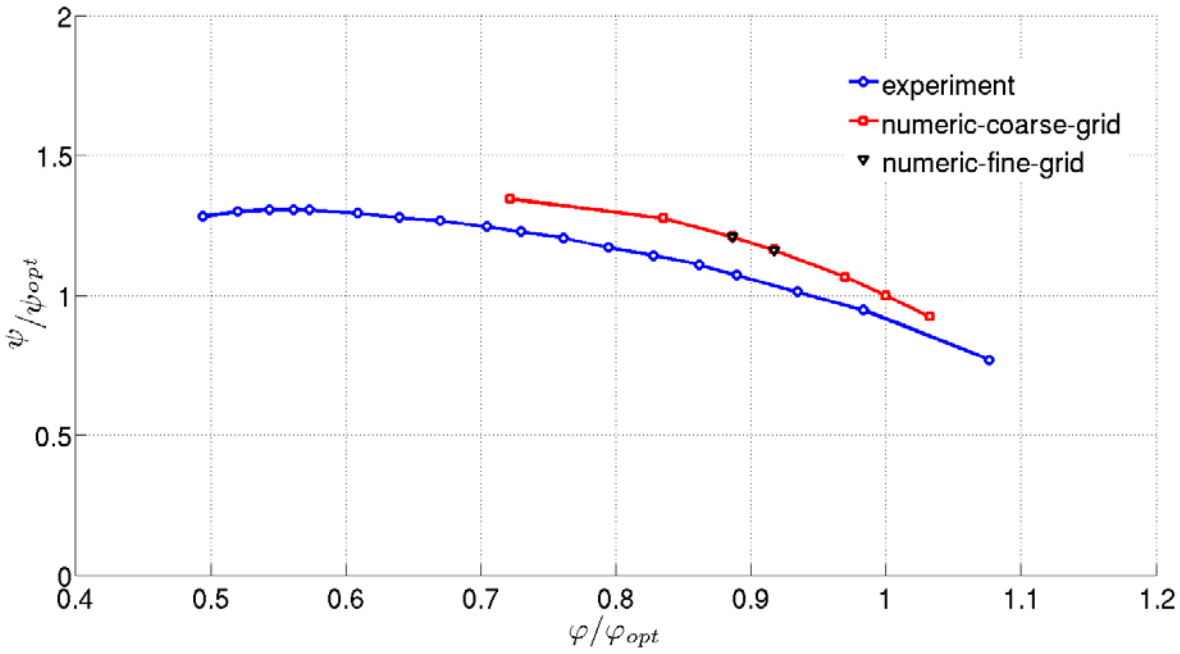

Figure 7. Total pressure rise

turbulence model). However this model has advantage in limited CPU time,

The second main part of this work is transient calculation. The calculated spectra show the correct blade sequence frequencies (f_z and its harmonics). Here the sound level is overestimated, because FW-H analogy is developed for sound radiation into the open field.

ACKNOWLEDGEMENTS

The authors appreciate the experimental data provided by Mr. Karstadt.

REFERENCES

[1] Ffowcs Williams J.E., Hawkings D.L., Sound arbitrary motion, Philos. T. Roy. Soc. A 264 (A1151) (1969) 321–342.

[2] Lighthill M.J., On sound generated aerodynamically, I: general theory, P. Roy. Soc. Lond. A Mat. 221 (1952) 564–587.

[3] T.-H. Shih, W. W. Liou, A. Shabbir, Z. Yang, and J. Zhu. A New k-epsilon Eddy-Viscosity Model for High Reynolds Number Turbulent Flows - Model Development and Validation. Computers Fluids, 24(3):227–238, 1995.

[4] I. Proudman. The Generation of Noise by Isotropic Turbulence. Proc. Roy. Soc., A214:119, 1952.

[5] N. Curle. The fluence of Solid Boundaries upon Aerodynamic Sound. Proceedings of the Royal Society of London. Series A, Mathematical and Physical Sciences, 231:505–514, 1955.

[6] Farassat, F. And Succi, G. P., The Prediction of Helicopter Rotor Discrete Frequency Noise, Vertica, Vol. 7, No. 4, pp. 309-320, 1983.

[7] Fluent User Guide for FLUENT 6.3, 2006

[8] B. E. Launder and D. B. Spalding. Lectures in Mathematical Models of Turbulence. Academic Press, London, England, 1972.

[9] S. Karstadt, Influence of the Tip Clearance on the Acoustic and Aerodynamic Characteristics of a Fan. Diploma Thesis, Department of Mechanical Engineering, Chair of Fluid Systems Technology, TU Darmstadt, Germany, 2008

[10] K. S. Brentner, Modeling Aerodynamically Generated Sound: Recent Advances in Rotor Noise Prediction, Presented at 38th Aerospace Sciences Meeting and Exhibit, AIAA 2000-0345, January 10-13, Reno, Nevada, USA, 2000.